

## Adonyi Welding Consultants

276 Hillshore Circle N., Longview, TX 75605

Phone: 903-235-5891 or 903-233-3918, FAX: 903-233-3901

E-mail: [AdonyiWeldingConsultant@gmail.com](mailto:AdonyiWeldingConsultant@gmail.com), Website: [www.AdonyiWeldingConsultant.com](http://www.AdonyiWeldingConsultant.com)

Date: September 10, 2010

To: xxxx

**Subject: X60 welded pipe field failure**

Dear xxxx

A piece of API X60 pipe 12.75" OD and 0.219" wall thickness was received for evaluation and root cause analysis for failure during hydrotesting.

Based on destructive testing of the sample and Fracture Mechanics calculations, it was found that testing was performed adequately, but the pipe failed due to excessive ID scarfing and the presence of pre-existing flaws in the longitudinal ERW weld centerline. The pipe wall thinned by up to 10% by the excessive scarfing likely yielded during hydro-testing and the final fracture initiated at ID surface gouges and non-metallic inclusions on the ID side at the weld centerline.

Additionally, sliding contact arcing and subsequent energy loss to the weld due to overheating were observed adjacent to the ERW weld, indicating process instabilities that probably contributed to entrapment of inclusions/lack of fusion.

Improvements in manufacturing practices and NDE techniques are recommended to avoid similar failures in the future. Specifically, improved ID scarfing, reducing power losses through improper HF welder contact arcing and improved NDE detection were recommended.

Regards,

Yoni Adonyi, Ph.D., P.E.  
Welding Engineering Consultant

## Background

The subject pipe reportedly failed during hydrotesting underground at 1750 psi after 10 minutes of being pressurized. According to the customer report, testing started at 7:05 am on 6/17/2010 and ended at 7:30 am when water burst to the surface from the pipe already buried underground. The test temperature was not reported, but it can be assumed to have been between 60-80 deg F. No injuries or other damage were reported.

From the pressure chart, it is unclear why did the failure take 10 minutes to occur, as the type of fracture is indicative of instant burst, not a gradual opening. It is also interesting to note that failure occurred at 8 psi away from the required testing pressure (i.e. 1750 instead of 1758 psi).

The 12.75" diameter X60 API pipe was made using HF welding from Heat #108697, see certificates attached. The actual chemical composition indicated that the pipe was made of a low-carbon (0.022%) steel composition microalloyed with V (0.038%) and Nb (0.054%). This actual chemistry was lower in carbon than the 0.05% C in the certificate, but very close in V and Nb to the aim values. This difference in Carbon content might have affected hardenability in the weld, but its significance in the failure is unclear.

Indeed, the weld hardness away from the fracture showed at the weld centerline a peak hardness on 245 HV, a bit high to be expected for this composition. Due to the relative small size of the weld, it can be assumed that the heat input was low and cooling rates high.

## Results and Discussion

A top view of the failed pipe is shown in Figure 1, showing evidence of classical fracture under Hoop stresses, initiating at the middle (Arrow), propagating in both direction (dashed line) and stopping when the driving force i.e, the internal pressure was relieved.

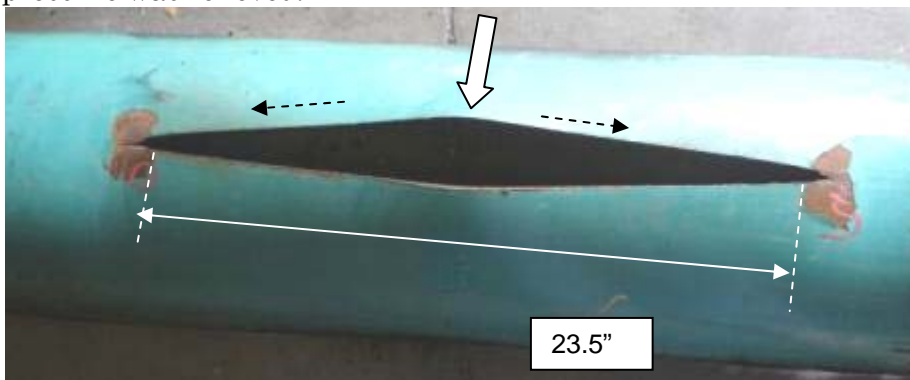


Figure 1. Top view of the pipe fractured during hydrotesting along the ERW weld line. The total crack length ( $2a=23.5''$ ) can be used in calculation of strain energy release, assuming a classical Griffith plane strain model).

Figure 2 shows one of the extremities of the fracture where the crack propagating along the ERW centerline stopped.



Figure 2. Crack arrest side O, with the paint peeled off around the plastic zone in front of the crack tip. This is typical of a classic Case I situation in Fracture Mechanics when the stress in front of the crack tip becomes lower than the yield strength, causing the crack to stop.

By comparing the approximate size of the above plastic zone with the theoretical value, we can estimate if the stresses developed during hydrotesting. Comparing the calculated stress intensity factor of the weld flaw with the fracture toughness, the critical size of the flaw can be established.

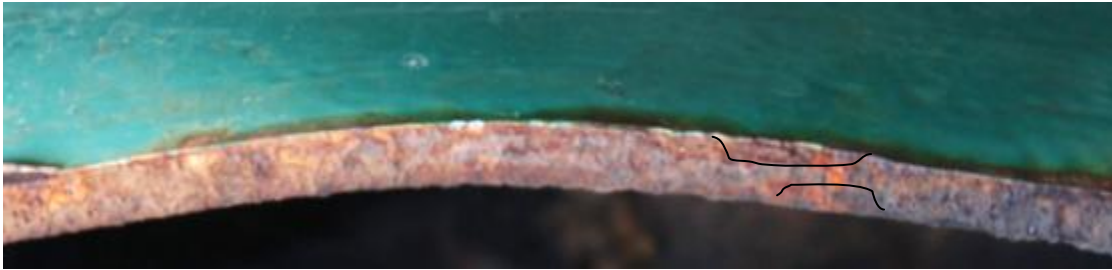
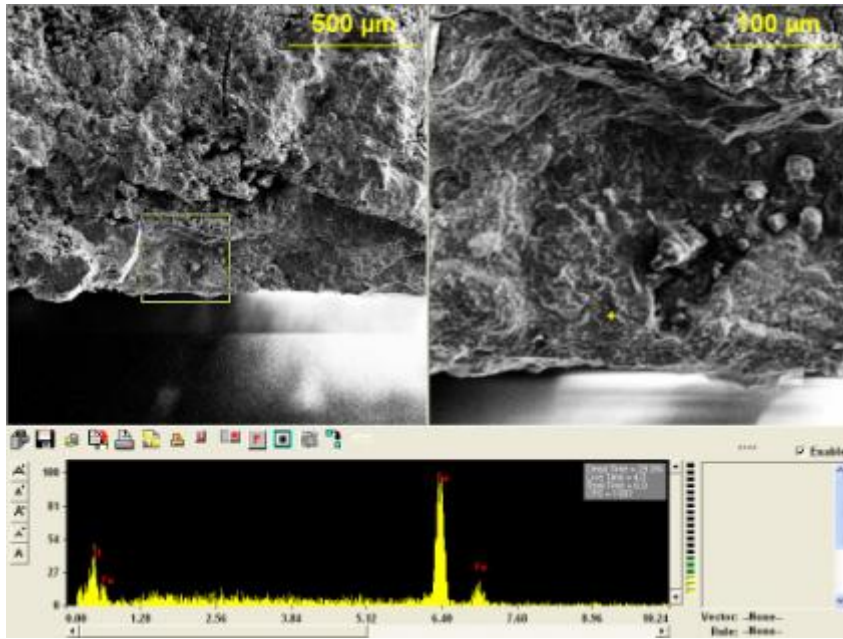
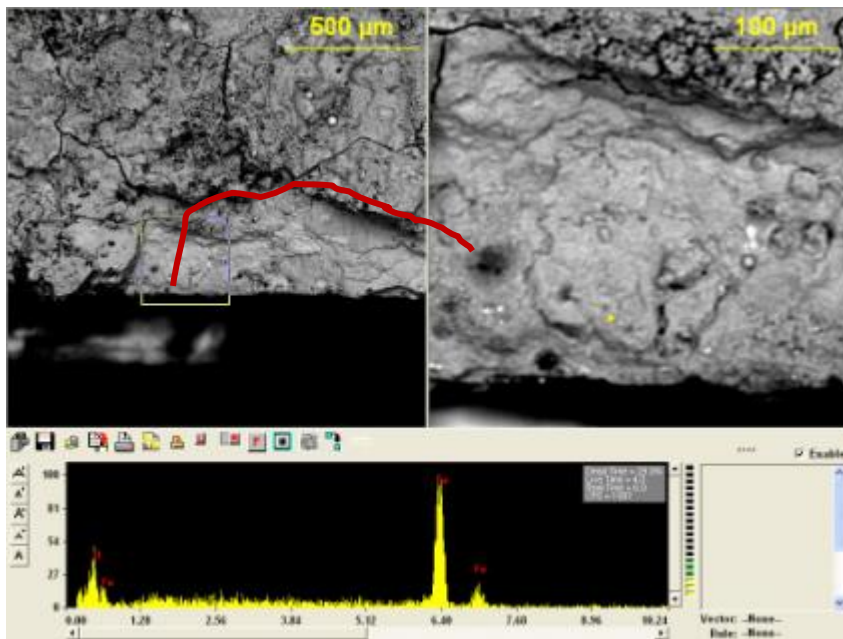


Figure 3. Multiple potential initiation/propagation sites on the weld ID and OD sides of the weld. Chevron marks on the fracture surface indicate sudden crack propagation in a single-event failure.

A close-up of some possible initiation sites were highlighted and sized relative to the wall thickness. One of the ID weld lack of fusion is shown in Figure 4.



(a)



(b)

Figure 4. Secondary Electron (a) and Backscattered Electron Imaging (b) of the ID initiation site – highlighted – covered with heavy Iron Oxide

Calculating the Hoop tensile stresses for the 1,750 psi at failure resulted in a stress of 54.71 ksi, which is less than the 69 ksi yield strength of the steel ( $\sigma = [P \cdot r] / t$ ). Therefore, a discontinuity had to be present to lower the strength of the

pipe wall. Indeed, the longitudinal ERW weld split along its centerline and several discontinuities were apparent at the initiation site, together with evidence of plastic deformation as well as thinning of the pipe wall due to excessive weld scarfing, Figure 5.

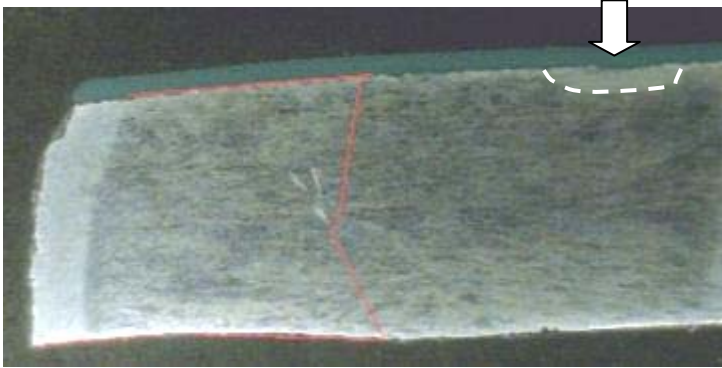


Figure 5. Transverse cross section through the initiation site, showing that the fracture occurred along the weld centerline, as well as evidence of thinning (see highlighted area 2.6 mm wide), 8.7 X magnification.

For this initial plastic deformation to occur (probably during the first 10 minutes of hydro-testing, as reported), the local stress must have exceeded the yield strength of the material (69 ksi). Evidence of plasticity was also found on the fracture surface, Figure 6, further supporting the initial yielding theory before the final sudden fracture.

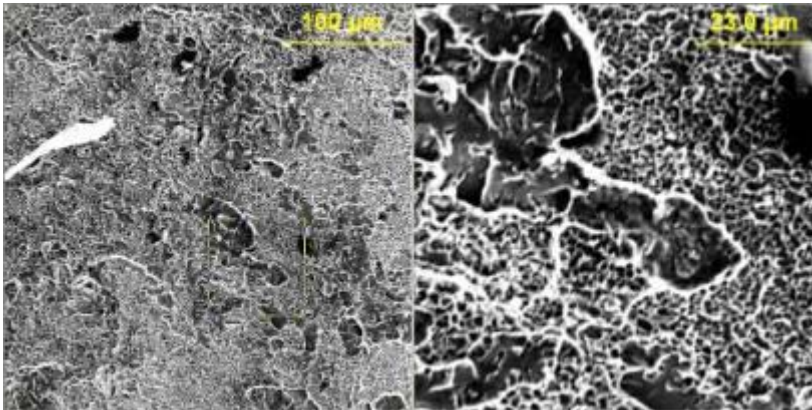


Figure 6. Ductile dimples on the fracture surface, ID toward mid-section area, confirming initial plasticity and deformation in the pipe, 1000 X magnification

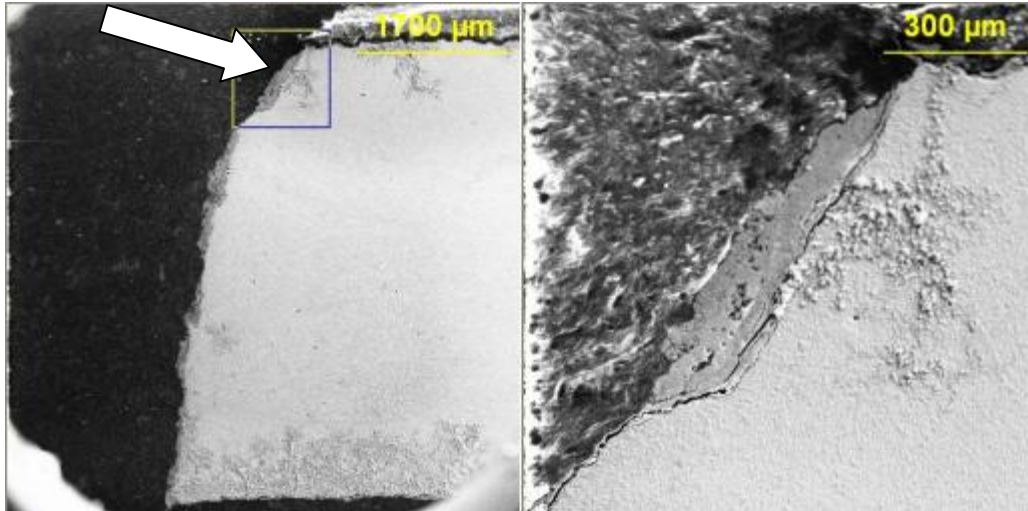


Figure 7. Close-up of the OD weld centerline oxide inclusion (arrow) that reduced the effective cross section resisting deformation, 90X magnification.

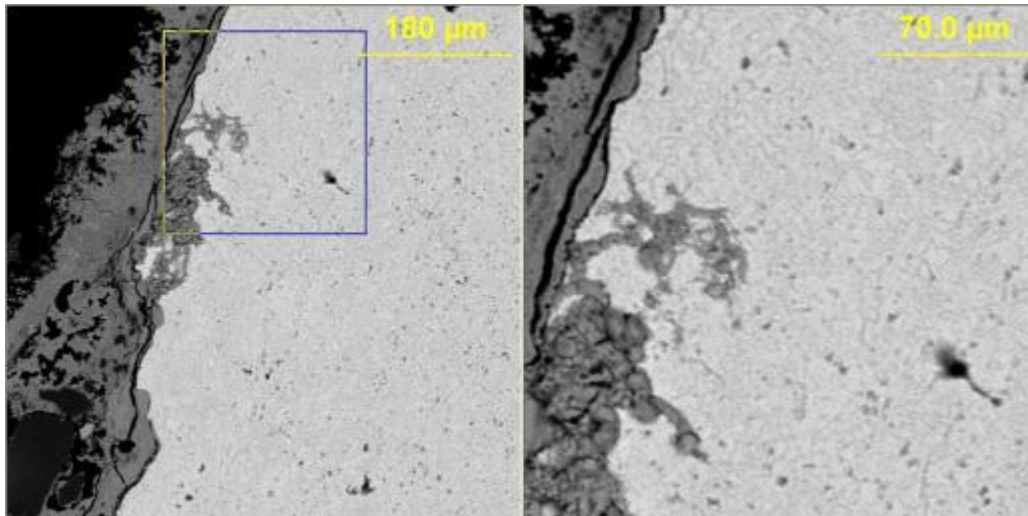


Figure 8. Morphology of the entrapped oxide at the weld centerline, 370 X magnification

Thus, the subsequent instant rupture type failure can be assumed to have started and propagated in an unstable crack propagation mode because the stress intensity factor  $K_I$  exceeded the critical weld fracture toughness  $K_{Ic}$  due to the presence of this flaw.

These possible initiation sites were removed, cleaned in ultrasonic bath and the fracture surface was examined in the SEM. The opposite side of the fracture was cross sectioned perpendicularly to the surface, mounted, polished and etched, together with a sample of the weld away from the fracture.

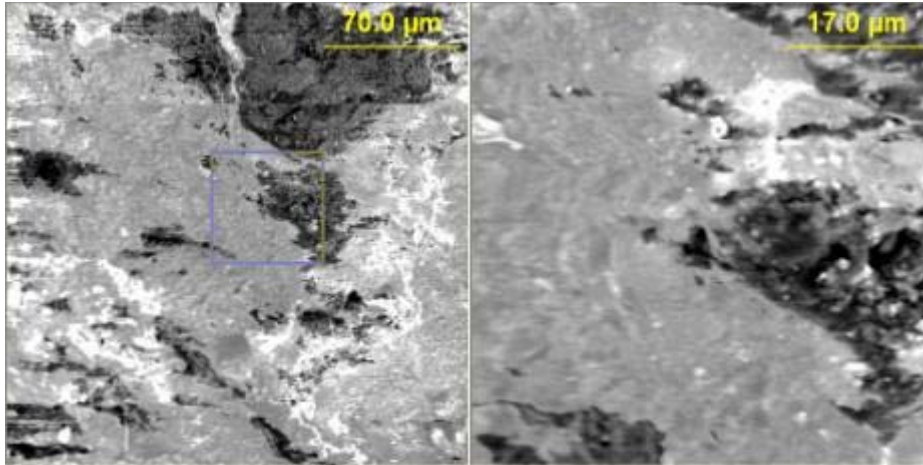


Figure 9. SEM view of the high temperature oxide on the fracture surface at the initiation site. Again, the flat surface of the entrapped oxide was likely the lack of fusion that initiated the final failure. These areas correspond to the top (OD side) of the cross section shown in Figure 5.

Finally, a random cross section was performed on the ERW weld away from the fracture site, Figure 10.

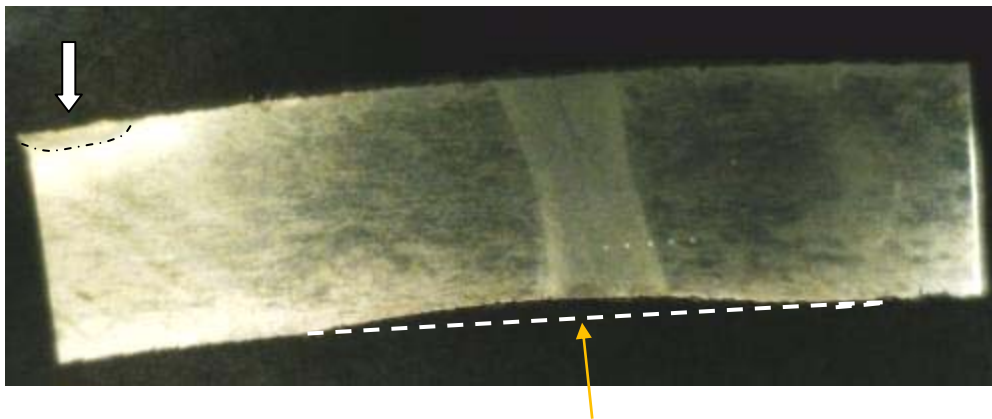


Figure 10. View of the ERW weld ~ 2 feet away from the failure area, 8.3 X magnification. Notice the excessive and asymmetrical ID scarfing that caused wall thinning of 0.6 mm or 9%, as well as the arc mark from the sliding contact, arrow, 2.35 mm wide arcing HAZ.

It is unclear what kind of weld parameter fluctuation produced the narrower arcing HAZ than in the area of the initiation site. Nevertheless, a tighter parameter control will be required in the future, including elimination of HAZ and sliding contact arcing.

A close-up at ID weld centerline revealed in cross section additional grooves (stress risers) left by inadequate scarfing, Figure 11, as well as a centerline inclusion line shown in Figure 12.

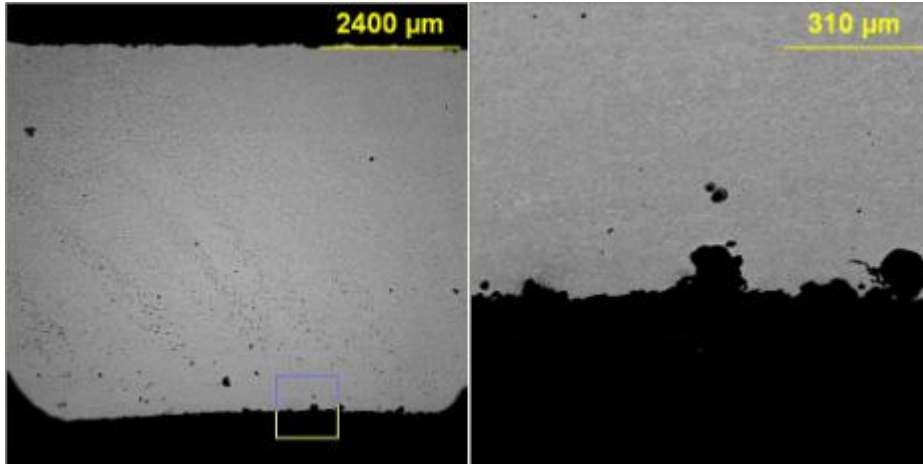


Figure 11. Longitudinal grooves left on the weld ID side by inadequate scarfing, possible initiation sites for failure under internal pressure because of stress concentration

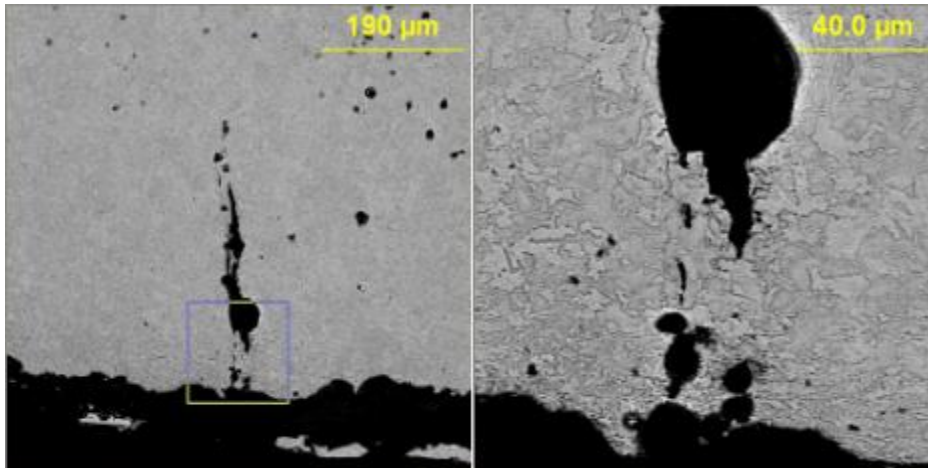


Figure 12. Internal lack of fusion along the weld centerline, the most likely cause for failure initiation, as shown in the fractograph in Figure 4.

## Conclusions

1. The pipe failed because of a combination of factors such as a) excessive and asymmetrical ID scarfing that thinned the pipe wall, and b) deep scarfing grooves that became stress risers. Finally, pre-existing linear centerline weld flaws were found at the initiation site at the ERW weld bondline. These resulted in initial yielding, followed by unstable crack growth.
2. The sliding electrical contact adjacent to the HF weld caused localized OD heating and loss of energy to the weld, resulting in a narrow and hard weld.
3. Improved weld process control, scarfing methods and better NDE methods will be needed to avoid similar failures in the future.

### **Recommendations**

While it is difficult to establish a priority list in remedial actions, all suggestions below are considered to be important enough to be addressed immediately:

1. Improve ID scarfing to avoid reducing the thickness in the weld area and eliminate gouges that act as stress risers. I believe NDE and metallography at the mill should have caught this problem after manufacturing.
2. Improve the NDE technique sensitivity, as the UT system should have certainly been caught during post-weld inspection
3. Improve High Frequency welding parameters to avoid internal inclusions in the future (better squeezout, improved welding cleanliness, etc).